

Design of Current-Type Readout Integrated Circuit for 160×120 Pixel Array Applications

Eun Sik Jung*, Young Seok Bae* and Man Young Sung[†]

Abstract – We propose a Readout Integrated Circuit (ROIC), which applies a fixed current bias sensing method to the input stage in order to simplify the circuit structure and the infrared sensor characteristic control. For the sample-and-hold stage to display and control a signal detected by the infrared sensor using a two-dimensional (2D) focal plane array, a differential delta sampling (DDS) circuit is proposed, which effectively removes the FPN. In addition, the output characteristic is improved to have wider bandwidth and higher gain by applying a two-stage variable gain amplifier (VGA). The output characteristic of the proposed device was $23.91 \text{ mV}/^\circ\text{C}$, and the linearity error rate was less than 0.22%. After checking the performance of the ROIC using HSPICE simulation, the chip was manufactured and measured using the SMIC 0.35 μm standard CMOS process to confirm that the simulation results from the actual design are in good agreement with the measurement results.

Keywords: Readout IC, Microbolometer, Infrared ray, Image sensor

1. Introduction

An infrared ray image device, which displays the image of an object by sensing the radiation energy emitted from the object, is composed of a sensor that detects thermal energy and converts it into an electric signal, an ROIC that processes the electric signal into the video signal appropriate for processing, and other signal-processing circuits [1]. Existing uncooled-type ROICs for infrared sensors are mainly designed with a fixed voltage bias in the input structure [2, 3]. In this paper, the input structure of the proposed fixed current-type ROIC is removed in the integrator to simplify its input structure compared to that of the conventional fixed voltage-type ROIC circuit. The proposed fixed current-type ROIC allows for the control of the current bias through the active bias characteristics of the bolometer pixel, which makes it easier to adjust the sensitivity and output characteristics of the ROIC. Furthermore, because the microbolometer used infrared sensitive material and was manufactured using the MEMS process, the characteristics of the bolometer can be changed by varying the process. Therefore, a DDS stage is proposed to compensate for the FPN [4]. The DDS stage receives the reference and active pixel signals and then saves the values, effectively reducing the noise that exists in both the reference and active signals through differential output in sequence. Lastly, gain is controlled to increase the stability of the noisy signal from the DDS by adding the VGA to the final output terminal of the ROIC. In

addition, the output signal of the ROIC is controlled, such that it is appropriate for the video processing system.

2. Structure of the Proposed ROIC

2.1 Circuit description and operation

Fig. 1 shows a block diagram of the proposed 160×120 pixel array controllable fixed current-type ROIC. The ROIC is composed of an input structure that was configured by connecting an active pixel array to respond to and change the infrared ray, and a reference pixel array that does not respond to the infrared ray in parallel. These pixels are connected in series to the current source to generate a voltage difference between the active pixel array and the reference pixel array. The input structure has a DDS stage to sequentially sample and hold the generated 160-column pixel signal, and a VGA that gives the proposed ROIC its wide bandwidth and high gain.

The signal-sensing mechanism used to detect the infrared ray is described as follows. When the infrared thermal energy is applied to a microbolometer pixel, the resistance of the bolometer pixel will change. At this time, when a bias is applied to the bolometer pixel, the voltage as – much as the changed resistance – is generated as an output signal. In the input stage, the microbolometer is arranged in a 160×120 array, and the reference bolometer pixel for each row is arranged in a 1×120 array. The active bolometer array is exposed to the infrared ray, and the reference bolometer is covered by a blind mask, unaffected by the infrared ray. Therefore, when the infrared ray is applied, the difference in resistance between the active

[†] Corresponding author: Department of Electrical Engineering, Korea University, Korea (semicad@korea.ac.kr)

* Department of Electrical Engineering, Korea University, Korea

Received: June 14, 2010; Accepted: September 26, 2011

bolometer and the reference bolometer is detected in the input stage. Hence, a controllable fixed current bias sensing method is applied to detect signal at the input stage.

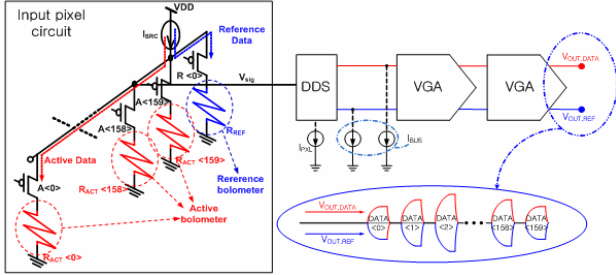


Fig. 1. Block diagram of the proposed 160×120 CMOS ROIC

As shown in Fig. 1, when the $R<0>$ switch of the input stage is turned on, the current source I_{SRC} and reference bolometer resistance element R_{REF} are connected to generate the voltage described by (1).

$$V_{REF-sig} = I_{SRC} R_{REF} \quad (1)$$

Similarly, when the $A<0>-A<159>$ switches are sequentially turned on, the active bolometer resistance R_{ACT} is connected to the current source to generate voltage as described by (2).

$$V_{ACT-sig} = I_{SRC} R_{ACT} \quad (2)$$

The signal sensed from the input stage is sent to the proposed DDS stage, which operates as the essential block to sample and hold the signal in the 2D focal plane array driving circuit, and effectively removes the FPN from the process variation by sampling the voltage differences between the two outputs of the reference and the active bolometer. Additionally, a 2D thermal image can be displayed by saving the 160-column data for each specific row of the input stage, and processing the signal by sending it to the VGA stage in order. The VGA stage amplifies the small and unstable DDS output to enhance the stability of the signal by applying the two-stage VGA using a rail-to-rail fully differential operational amplifier. Moreover, the gain is not fixed because the signal-sensing level changes according to the bias characteristics of the active bolometer. By adding a VGA stage that is not fixed and can be controlled, the final output signal of the ROIC can be controlled.

2.2 DDS and VGA stage operation

Fig. 2 shows the circuit structure of the DDS and VGA stage. When $V_{REF-sig}$, which is the reference bolometer signal of the input stage as shown in (1), is sent to the M_1 gate, the switch S_1 is turned on to pass the signal through

to the source follower composed of transistor M_1 .

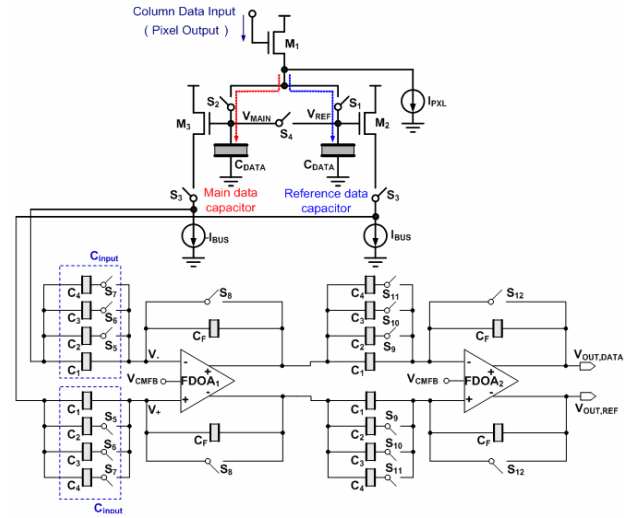


Fig. 2. Circuit diagram of the proposed DDS and VGA stage

As it passes through the source follower, the DC-level shifted voltage is saved to the output signal data storage capacitor C_{DATA} . The reference bolometer signal is disconnected after the reference bolometer output signal is stored, and an active bolometer output signal $V_{ACT-sig}$, as described by (2), is sent to the M_1 gate. At this time, switch S_2 is turned on and the DC-level shifted voltage is saved to C_{DATA} after passing through the source follower containing M_1 . V_{REF} and V_{MAIN} , which are saved on C_{DATA} in the DDS stage, once again pass through the source follower when switch S_3 is turned on to generate voltage outputs to the negative and positive terminals of the VGA stage, as shown in (3) and (4), respectively.

$$V_+ = V_{REF} - V_{GS2} \quad (3)$$

$$V_- = V_{MAIN} - V_{GS3} \quad (4)$$

Where V_{REF} and V_{MAIN} are defined in (5) and (6), respectively:

$$V_{REF} = V_{REF-sig} - V_{GS1} \quad (5)$$

$$V_{MAIN} = V_{ACT-sig} - V_{GS1} \quad (6)$$

The change in bolometer resistance due to the irradiation of the infrared ray is proportional to the voltage difference between $DDS_{REF-out}$, which is the DDS reference output, and $DDS_{DATA-out}$, which is the DDS data output, as described by (7).

$$\begin{aligned} V_{DATA} &= DDS_{REF-out} - DDS_{DATA-out} \\ &= R_{REF} \cdot I_{SRC} - (R_{REF} - \Delta R) \cdot I_{SRC} \\ &= \Delta R \cdot I_{SRC} \end{aligned} \quad (7)$$

Where ΔR is the resistance variation of the bolometer due to the infrared ray. As shown in (7), the FPN can be removed efficiently because V_{DATA} outputs the voltage difference between $DDS_{REF-out}$ and $DDS_{DATA-out}$. If the FPN is assumed to be R_{FPN} , the output of the DDS stage can be represented by (8).

$$\begin{aligned} V_{DATA} &= DDS_{REF-out} - DDS_{DATA-out} \\ &= (R_{REF} + R_{FPN}) \cdot I_{SRC} - (R_{REF} + R_{FPN} - \Delta R) \cdot I_{SRC} \quad (8) \\ &= \Delta R \cdot I_{SRC} \end{aligned}$$

Therefore, as shown in (8), FPN is cancelled by applying the proposed DDS stage. When switch S_4 is turned on, the gate voltages of M_2 and M_3 become the average value of V_{MAIN} and V_{REF} . The VGA stage forms a feedback loop with a capacitor between the input and output terminals of the fully differential operational amplifier. The closed loop gain of the VGA, A_{closed} , is given by (9).

$$A_{closed} = \frac{C_{input}}{C_F} \quad (9)$$

The capacitor of the VGA is connected to the switch, and the gain of the first VGA stage is confirmed through a signal generated based on switches S_5 , S_6 , and S_7 from the external digital terminal. After the input signal is amplified and switch S_8 is turned on, the input and output are shorted to convert the output of the first VGA stage to V_{CMFB} . At this time, the output pulse of the first VGA stage becomes the input signal of the second VGA stage to be amplified by the confirmed gain from the signal based on switches S_9 , S_{10} , and S_{11} from the external digital terminal. As previously mentioned, the gain variation can be improved by connecting the two VGA stages in series.

3. Simulation Results and Chip Test

The output characteristic of the proposed 160×120 pixel array controllable fixed current-type ROIC was simulated using HSPICE. Table 1 shows the output characteristic condition of the reference and the active bolometer during simulation, where the output characteristics of the manufactured thin amorphous silicon microbolometer pixel were applied. The output characteristic of the ROIC is shown in Fig. 3.

The red waveform in the figure shows the output terminal voltage $V_{OUT,DATA}$, while the blue waveform shows the output terminal voltage $V_{OUT,REF}$ from Fig. 2. According to the data shown in Fig. 3, the output results can be summarized as 362.24 mV at 10°C, 190.11 mV at 20°C, -6.91 mV at 30°C, -230.12 mV at 40°C, and -510.87 mV at 50°C. Fig. 4 shows our analysis of the output signal and the linearity error rate when the temperature changes in

Table 1. Simulation conditions

Parameter	Value
R_{REF}	1 M Ω @ 30°C
R_{MAIN}	1.02007 M Ω @ 10°C
	1.01066 M Ω @ 20°C
	1.00000 M Ω @ 30°C
	0.98783 M Ω @ 40°C
	0.97253 M Ω @ 50°C
VGA gain capacitance	$C_1 = 0.6$ pF
	$C_2 = 0.6$ pF
	$C_3 = 1.2$ pF
	$C_4 = 2.4$ pF
	$C_F = 0.3$ pF

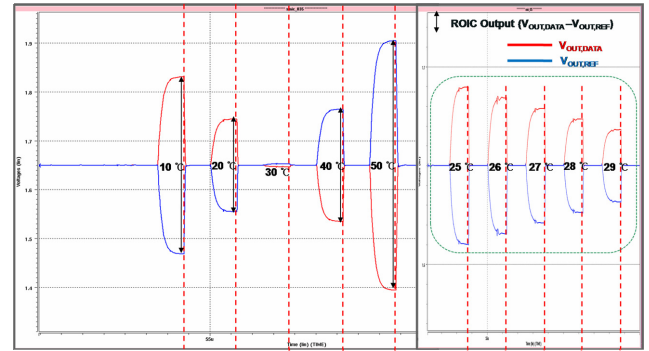


Fig. 3. Output characteristics of the VGA stage

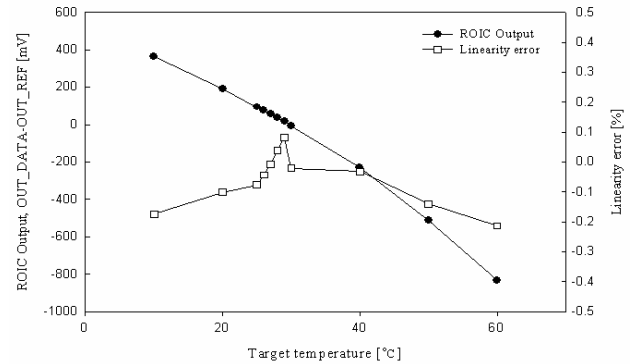


Fig. 4. The characteristics of the linearity error of the proposed ROIC

the range of 10–50°C. The proposed ROIC has a signal-sensing level of 23.91 mV/°C when the voltage gain of the VGA is 64 V/V. The linearity error rate was less than 0.22%, indicating the good linearity of the output characteristics. The chip was manufactured based on the SMIC 0.35 μ m standard CMOS process to check the performance of the proposed ROIC. The measured condition is the same as the simulation condition. Figs. 5 and 6 show the test board and the waveform results of the chip test, respectively.

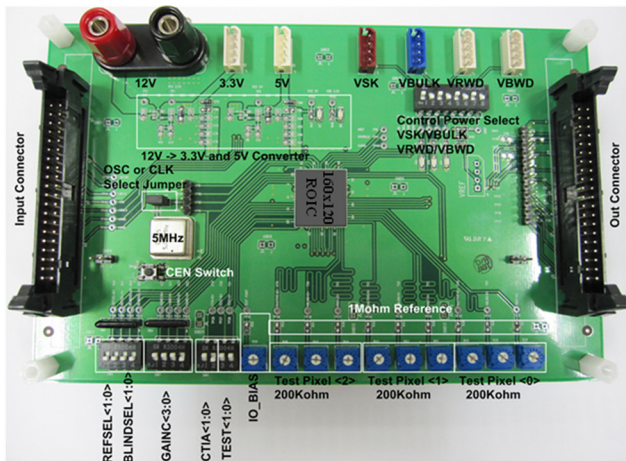


Fig. 5. Test board for the proposed ROIC

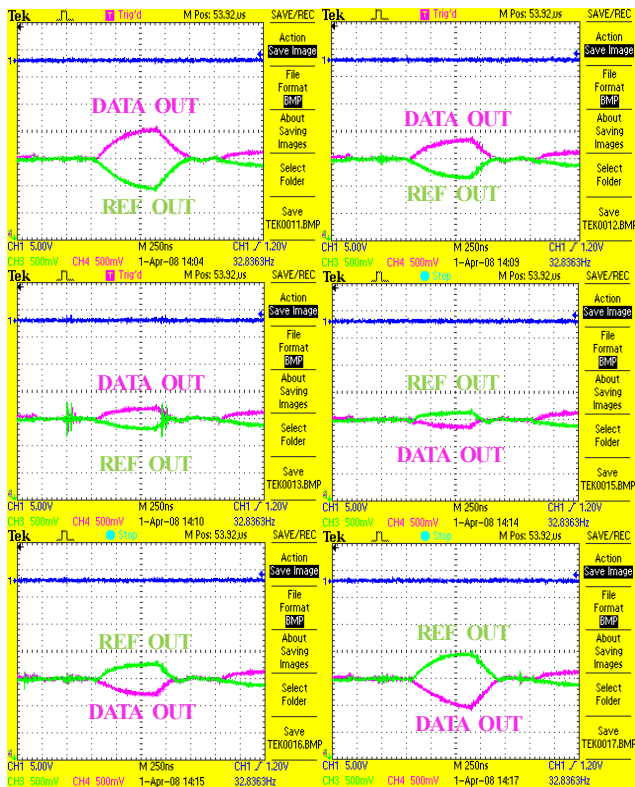


Fig. 6. Chip test results of the proposed 160×120 CMOS ROIC

4. Conclusion

We proposed a controllable fixed current type ROIC with high signal gain, good noise immunity, and excellent output characteristics. Based on the HSPICE simulation, the proposed ROIC appeared to compensate for errors caused by bolometer and reference resistance variation with process variation. The proposed circuit was manufactured to confirm that it operates as designed, as shown by the results of the validation test.

References

- [1] F. Niklaus, A. Decharat, C. Jansson and G. Stemme, "Performance model for uncooled infrared bolometer arrays and performance predictions of bolometers operating at atmospheric pressure", *Infrared Phys. Technol.* vol. **51**, no. 3, pp. 168-177, (2008).
- [2] S.-J. Hwang, H.-H. Shin and M.-Y. Sung, "A New CMOS Read-out IC for Uncooled Microbolometer Infrared Image Sensor", *Int. J. Infrared Millimeter Waves*, vol. **29**, no. 10, pp. 953-965, (2008).
- [3] C. Heish, C. Wu, F. Jih and T. Sun, "Focal-Plane Arrays and CMOS Readout Techniques of Infrared Imaging Systems", *IEEE Trans. Circuits System for Video Technol.* Vol. **7**, no. 4, pp. 594-605 (1997).
- [4] S. K. Mendis, S. E. Kemeny, R. C. Gee, B. Pain, C. O. Staller, Q. Kim and E. R. Fossum, "CMOS Active Pixel Image Sensors for High Integrated Imaging Systems", *IEEE J. Solid State Circuits*, vol. **32**, no. 2, pp. 187-197, (1997).



Eun Sik Jung He is taking up his Ph.D in Electrical Engineering from Korea University. His research interests include readout integrated circuit for uncooled IR detector and high-voltage power devices.



Young Seok Bae He is currently a Master's course student in Korea University. His research interests include electrostatic discharge (ESD) and analog circuit design



Man Young Sung He received his M.S. and Ph.D degrees in Electrical Engineering from Korea University in 1977 and 1981, respectively. He is currently the Dean of the College of Engineering at Korea University. He was with the University of Illinois at Urbana-Champaign as an associate professor in 1986 and as a visiting professor in 1997, and with the Royal Institute of Technology (Sweden) as a visiting scientist in 1991. His research interests include power devices based on silicon and compound semiconductors, and smart power IC design